THE ASTROPHYSICAL JOURNAL, 563:L173–L177, 2001 December 20

ACTIVE REGION TRANSIENT EVENTS OBSERVED WITH *TRACE*

DANIEL B. SEATON, AMY R. WINEBARGER, EDWARD E. DELUCA, LEON GOLUB, AND KATHARINE K. REEVES
Harvard-Smithsonian Center for Astrophysics, 60 Garden Street, Cambridge, MA 02138; dseaton@cfa.harvard.edu, awinebarger@cfa.harvard.edu, edeluca@cfa.harvard.edu, lgolub@cfa.harvard.edu, kreeves@cfa.harvard.edu
AND
PETER T. GALLAGHER[1]
Big Bear Solar Observatory, New Jersey Institute of Technology, 40386 North Shore Lane, Big Bear City, CA 92314; ptg@bbso.njit.edu
Received 2001 October 25; accepted 2001 November 16; published 2001 December 12

ABSTRACT

Nearly all active region observations made by the *Transition Region and Coronal Explorer* (*TRACE*) contain seemingly spontaneous, short-lived brightenings in small-scale loops. In this paper, we present an analysis of these brightenings using high-cadence *TRACE* observations of Active Region 9506 on 2001 June 21 from 15:17:00 to 15:46:00 UT. During this time frame, several brightenings were observed over a neutral line in a region of emerging flux that had intensity signatures in both the 171 Å (log $T_e \approx 6.0$) and 1600 Å (log $T_e \approx 4.0$–5.0) channels. The events had a cross-sectional diameter of approximately 2″ and a length of 25″. We interpret these as reconnection events associated with flux emergence, possible EUV counterparts to active region transient brightenings.

Subject headings: Sun: activity — Sun: corona

On-line material: color figures

1. INTRODUCTION

Over the last two decades the increased sensitivity of solar instrumentation has allowed observations of small flarelike transient events in the solar corona. Shimizu (1994) discovered short-lived brightenings of compact (10–100 Mm) loops in Soft X-Ray Telescope (SXT) observations of active regions. These moderate energy (10^{25}–10^{29} ergs) events, called active region transient brightenings (ARTBs), often coincided with the hard X-ray microflares (Lin et al. 1984). The lifetimes of these events range from a few to tens of minutes, with between 1 and 40 events occurring per active region per hour (Shimizu 1994). The loops that brightened were either in emerging flux regions or on the outer edge of large spots (Shimizu et al. 1996). SXT temperature ratios give a maximum temperature range of about 2–8 MK for these events (Berghmans, McKenzie, & Clette 2001).

Similar transient brightenings have been observed in high-cadence EUV images taken with the EUV Imaging Telescope (EIT; Berghmans & Clette 1999). The observed EUV brightenings most often occurred in the core of active regions, with as many as 1 event per 10 s in a given active region (Berghmans & Clette 1999). The areas of the brightenings were between 10 and 100 Mm^2, and the durations were between 1 and 15 minutes (Berghmans & Clette 1999). In a comparison between the EUV and SXT events, it was found that some correspondence existed, although it was not one-to-one (Berghmans et al. 2001). Some events, typically the largest ARTBs, had a cospatial EUV event, while others were not correlated (Berghmans et al. 2001). In the EUV events that were cospatial with the SXT events, the peak in the EUV intensity occurred before the peak in the SXT intensity (Berghmans et al. 2001).

In this paper, we continue the study of transient active region brightenings by presenting *TRACE* observations of active region 9506 in two bandpasses: 171 Å (Fe IX/X at $T \sim 10^6$ K) and 1600 Å (continuum and C IV at $T \sim 10^4$–10^5 K). We find that compact loops brighten in both channels nearly simultaneously, with the 1600 Å channel leading the 171 Å channel by ~20 s. The brightenings are short-lived, with a typical lifetime of a few hundred seconds. They occur over a neutral line in the active region and are associated with emerging magnetic flux. Because the intensity in the 1600 Å channel peaks before the intensity in the 171 Å channel, and because the timescale of the events is greater than their characteristic cooling time, we interpret these brightenings as loops that are heating through the (narrow) *TRACE* bandpass. This interpretation appears to agree with the previous observation that EUV intensity peaks before SXT intensity.

2. DATA AND ANALYSIS

The *Transition Region and Coronal Explorer* (*TRACE*) has been described in detail by Handy et al. (1999), Schrijver et al. (1999), and Golub et al. (1999). On 2001 June 21, *TRACE* observed NOAA 9506 between 15:00:00 UT and 15:46:00 UT. The observing sequence included 171 Å (Fe IX/X at log $T \approx 6.0$) and 1600 Å (continuum and C IV at log $T \approx 4.0$–5.0) images taken at a cadence of 35 s. Only three-fourths of the detector was read, giving a total field of view of 384″ × 384″. A full-disk EIT 171 Å image taken at 17:30:14 UT on 2001 June 21 is shown in the left panel of Figure 1. EIT is described in detail by Moses et al. (1997). The *TRACE* field of view is highlighted in this image by the solid line. NOAA 9506 was classified as beta-gamma on 2001 June 21, and proceeded to decay from this date on. It also produced a solitary C2.5 at 01:17 UT on June 21 and remained inactive thereafter.

The Michelson Doppler Imager (MDI), discussed in Scherrer et al. (1995), on board *SOHO* provided a set of high-resolution magnetograms taken at the same time as our *TRACE* observations. The magnetograms analyzed here were obtained from 15:17 UT to 16:00 UT on 2001 June 21 with MDI in high-resolution mode. In this mode, 10′ × 10′ images with a spatial resolution of ~2″ were taken simultaneously with *TRACE*.

Ignoring images for which there is no MDI coverage, a total of 44 of the *TRACE* 171 Å and 45 *TRACE* 1600 Å images have been analyzed from this sequence. Each 171 Å

[1] Current address: Emergent Information Technologies, Inc., NASA Goddard Space Flight Center, Code 682.3, Greenbelt, MD 29771.

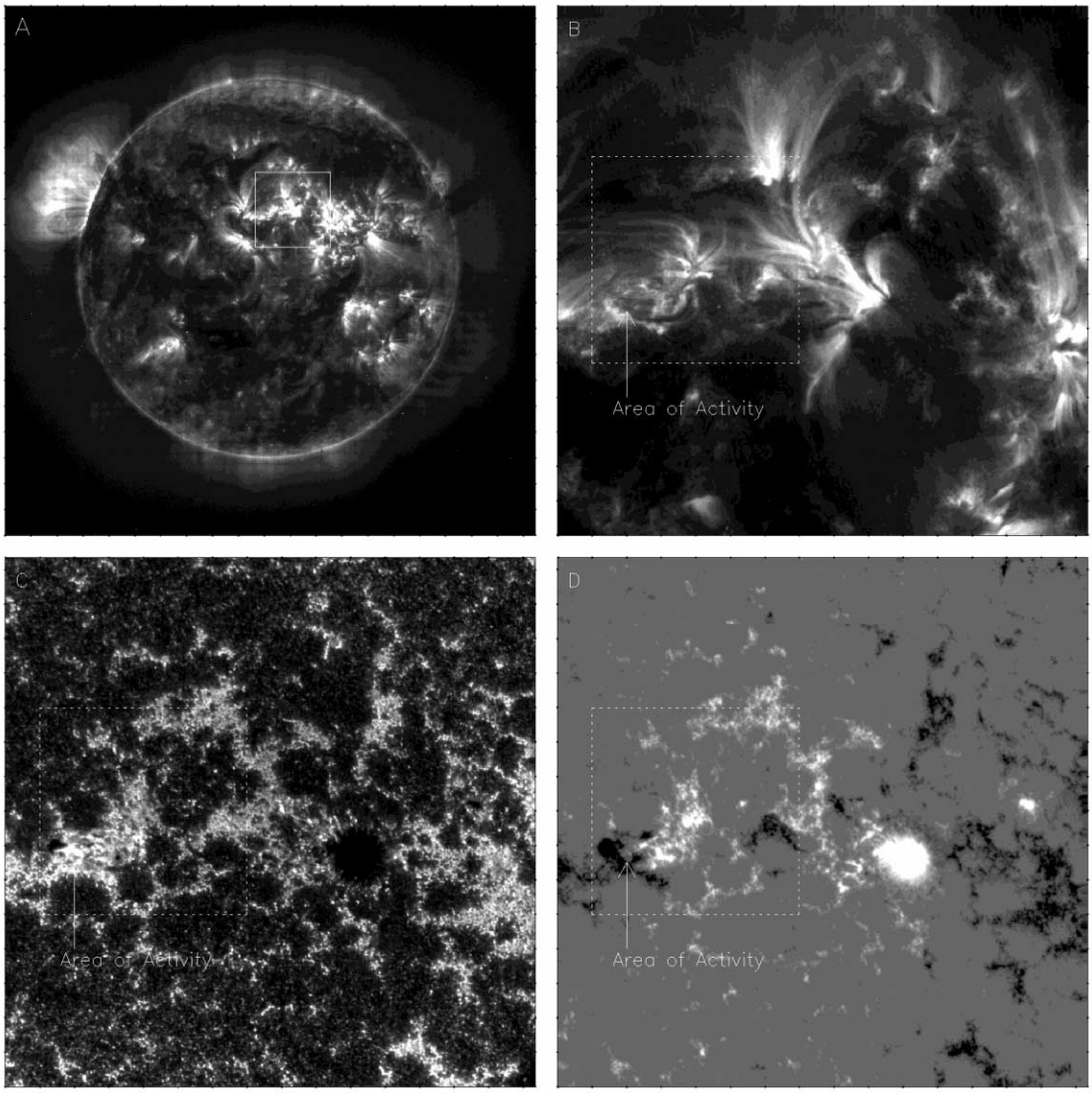

FIG. 1.—(*a*) EIT 171 Å image taken at 17:30:14 UT. The full *TRACE* field of view (panels *b* and *c*) is indicated by the solid line in the EIT image. (*b*) Full-field *TRACE* 171 Å image taken at 15:07:22 UT. (*c*) Full-field *TRACE* 1600 Å image taken at 15:04:43 UT. (*d*) MDI image, taken at 15:20:35 UT. In panels *b*, *c*, and *d*, the specific image area analyzed in this paper is highlighted by the dashed line. The particular area of activity is also indicated. [*See the electronic edition of the Journal for a color version of this figure.*]

image had an exposure time of 11 s, with the average count rate of ~2 DN s^{-1} $pixel^{-1}$, while each 1600 Å image had an exposure time of 0.9 s and the average count rate of ~150 DN s^{-1} $pixel^{-1}$. Example *TRACE* 171 and 1600 Å images are shown in Figures 1*b* and 1*c*, respectively, while a co-aligned MDI image is shown in Figure 1*d*.

Movies of this region (constructed by co-aligning the *TRACE* images, normalizing the flux to units of DN s^{-1}, and removing the impacts of radiation particles from the data) show that certain loops both appear and disappear in the 171 and 1600 Å channels over the duration of observation. These loops are compact, short lived, and clustered in the highlighted area indicated in Figure 1; they cross the neutral line in photospheric magnetic field.

To locate the best loop candidates for more detailed study, we employ a technique developed by Schrijver (2001). We create a data cube that contains the aligned and normalized 171 or 1600 Å *TRACE* images. Then, for each *TRACE* pixel, we find the median and maximum intensity over the period of observations. Finally, we generate an image of the maximum intensity minus the median intensity at every pixel. If the intensity in a pixel was fairly constant over the time frame, then we expect little contribution from that pixel in the subtracted image. However, if a pixel brightened for a short amount of time during that time frame, the subtracted image will be bright. The generated 171 and 1600 Å images are shown in Figure 2.

This method will locate all pixels that suffer intensity fluctuations during our observation time. There are many reasons why the intensities in a pixel could change over the observation time, such as heating, flows, transverse motions of loops, footpoint brightenings, etc. Examples of these are seen in this figure. However, there are two regions in this image that show loop brightenings that are cospatial in both the 171 and 1600 Å channels; they are labeled "multiple loop brightenings" and "single loop brightening" in Figure 2.

In the multiple loop brightening, a cluster of several loops all brighten at some point between 15:32:30 and 15:40:45 UT. This event clearly involved at least four separate loops. Be-

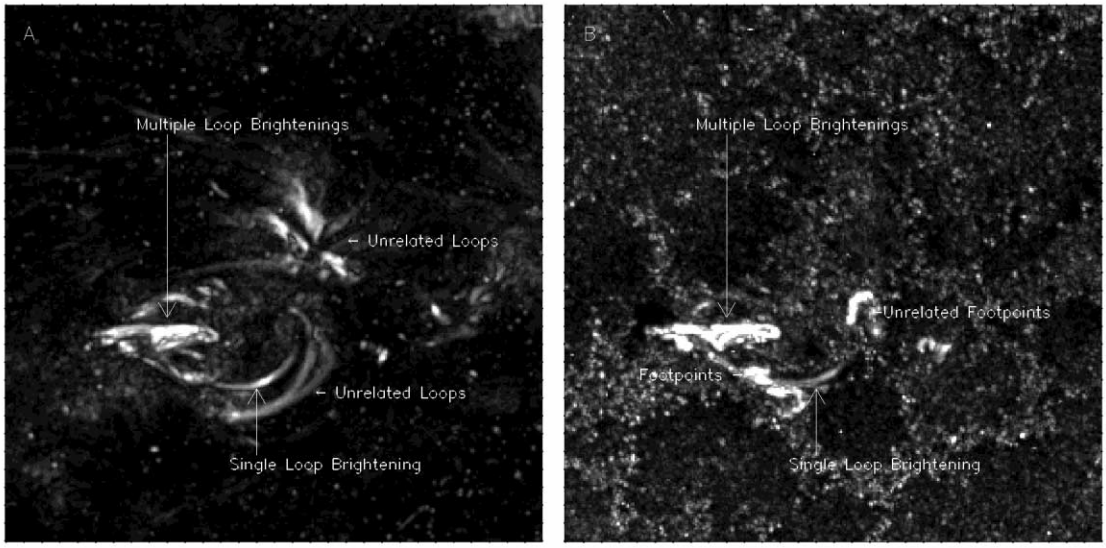

FIG. 2.—Panel *a* shows the dynamic activity in the *TRACE* 171 Å images, while panel *b* shows the dynamic activity in the *TRACE* 1600 Å images, making clear the areas that brightened in both 171 and 1600 Å. The two loop brightening events discussed in this paper are indicated by arrows in both images. Some loops brightened in 171 Å but not in 1600 Å and are pointed out as unrelated loops. Likewise, some footpoint activity occurred in the 1600 Å images and is indicated as well. [*See the electronic edition of the Journal for a color version of this figure*.]

cause the cluster is both dense and complex, with several overlapping loops and some loops that brighten, dim, and brighten again in that period, it is difficult to determine the beginning and end of most of the individual loop brightenings. Light curves taken over different areas of the cluster generally show the 1600 Å emission peaking shortly before the 171 Å emission. However, they often show several localized peaks, suggesting that the emission detected may come from a combination of overlapping loops. Figure 3 shows the evolution of a small area of the multiple loop brightening. The top row shows the 1600 Å emission and bottom row shows 171 Å emission, both between UT 15:34 and UT 15:38. We see that the loops brighten as a whole, without substantial footpoint brightening preceding the event, and that several connected and overlapping loops brighten during the event. The other region is a single (isolated) loop brightening, which is described below. Figure 4*a* shows the average curve for a small area of the loop cluster. Here, as in other parts of the cluster, the time profile of the 1600 Å emission completely envelops the 171 Å emission.

The single loop brightening had a cross-sectional diameter of approximately 2″ and length of 25″. Examination of the evolution of the light curves of the loop in 171 and 1600 Å, plotted spatially along the loop, showed that, within the cadence of observations, the loop brightens as a whole, as opposed to a single footpoint brightening that propagates along the loop. The peak intensity minus background in 171 Å is approximately 6 DN s^{-1} $pixel^{-1}$, and in 1600 Å is approximately 400 DN s^{-1} $pixel^{-1}$. Plotting the average flux of the entire loop versus time (Fig. 4*b*) reveals that the intensity in the 1600 Å band peaks at least 20 s before the peak intensity in 171 Å occurs, while the entire event takes ~300 s.

From MDI magnetogram movies of NOAA 9506, it is clear that there are several small-scale flux emergences close to both ends of the loop cluster identified in Figure 2. This is demonstrated in Figure 4*c* (multiple loop brightening) and Figure 4*d* (single loop brightening). The curves show the magnetic flux as a function of time averaged over the areas at the loop footpoints. As can be seen, the flux increases by about a factor of 3 (from ~25 to ~75 G) in 20–30 minutes, starting almost simultaneously with the 171 and 1600 Å passband brightenings. In addition to revealing the changes in magnetic field as the event progresses, the magnetograms show the loops' location, straddling the neutral line in the active region.

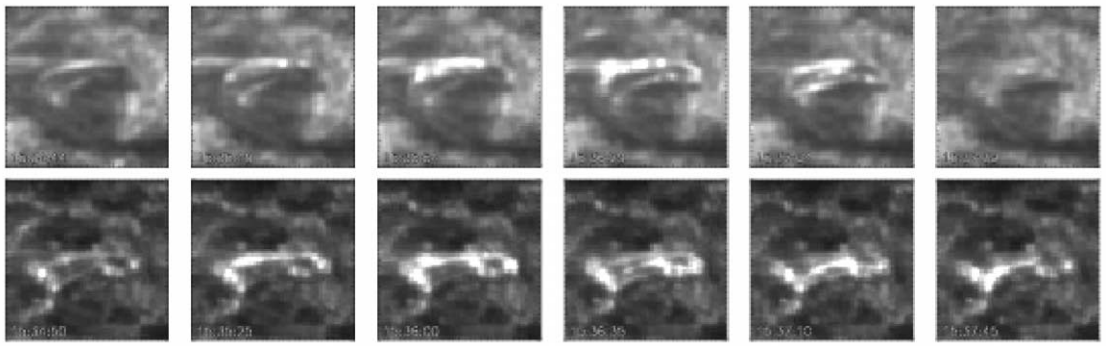

FIG. 3.—Evolution of loop brightenings in the corona, chromosphere, and photosphere. The top row shows the 171 Å passband emission between 15:34 and 15:37 UT, while the bottom row shows the 1600 Å passband (15:34–15:27 UT). [*See the electronic edition of the Journal for a color version of this figure*.]

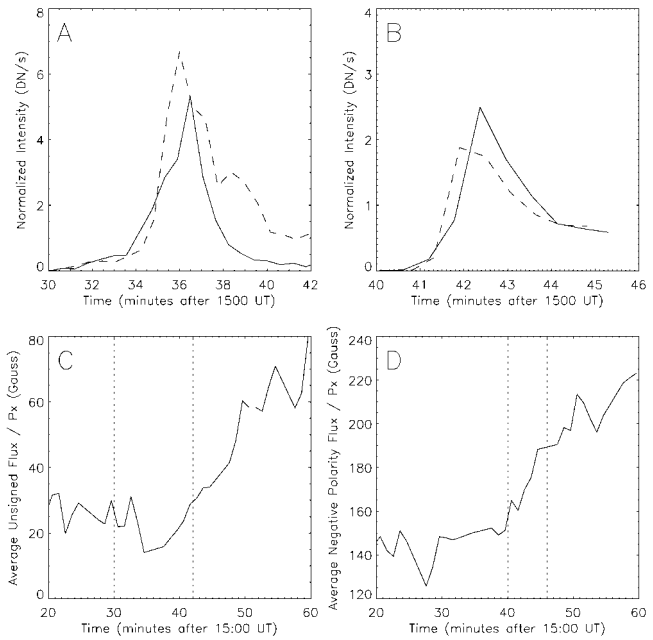

FIG. 4.—Average light curves and magnetic flux during transient events. (*a*) Average light curve in DN s^{-1} for one small region involved in the loop cluster event for both 171 Å (*solid line*) and 1600 Å (*dashed line*). (*b*) Average light curve in DN s^{-1} for the single loop event for both 171 Å (*solid line*) and 1600 Å (*dashed line*). For both light curves, the 1600 Å emission is scaled down by a factor of 100 in order to be shown on the same axes as the 171 Å intensity. (*c*) Average unsigned magnetic flux (Gauss) near the footpoints of the loops involved in the loop cluster event. (*d*) Average negative polarity magnetic flux at one of the footpoints of the single loop event. The vertical lines in (*c*) and (*d*) shows the time ranges covered by their counterparts in (*a*) and (*b*).

3. DISCUSSION

In this Letter, we have presented analysis of transient brightenings of compact loops observed in both the *TRACE* 171 Å and 1600 Å channels. The events were confined to the area over the neutral line in a region of emerging flux. In the one isolated example of a loop brightening, the 1600 Å intensity peaked approximately 20 s before the intensity in 171 Å, while in the loop cluster 1600 Å emission completely enveloped the 171 Å emission.

Previous analyses of EUV transient brightenings have detected the events based on an increase above a background intensity in a light curve for an individual pixel (Berghmans & Clette 1999). They found that transient brightenings could occur as frequently as 1 event per 10 s in a given active region. Our detection scheme required both an increased intensity above an average intensity and a cospatial signature in both the 171 and 1600 Å channels. Therefore, the events analyzed in this paper are only a small subset of the total events analyzed in previous work.

Because of the similarity in size, frequency and location, as well as the peak intensity in 1600 Å preceding the peak intensity in 171 Å, we believe *TRACE* is imaging the ARTBs as they are being heated by footpoint reconnection. This is significant because the 1600 Å channel has a strikingly different signature from the 1600 Å channel during a "classical" flare heated by loop-top reconnection. In the classical flare model, loop-top reconnection causes high-energy particles to stream down field lines and heat the chromospheric plasma (Forbes & Acton 1996). This causes increased emission in the 1600 Å channel at the footpoints of the flare long before the cooling, postflare loops appear in the *TRACE* 171 Å channel (Warren et al. 1999). In these events, the emission from 1600 Å is not confined to the loop footpoints. Instead, it fills the loops entirely within a single observing cycle (35 s). For a 10 Mm loop, this observations implies flows along the loop of ~300 km s^{-1}. Studying these events, then, puts important constraints on the energy release and plasma response during footpoint reconnection.

Because 1600 Å emission precedes 171 Å emission, we interpret these events as heating events. Why, then, do we not see them cooling? Using the SXT filter pair ratio, we can deduce that the ARTBs observed by SXT range in temperature from 2 to 8 MK (Shimizu 1994; Berghmans et al. 2001). Since, for the single loop event, we see the loop brighten in the cooler 1600 Å band and then the 171 Å band 20 s later, we might conclude that we have seen the loops warm through a temperature of $\sim 10^4$–10^5 K to a temperature of $\sim 10^6$ K. Furthermore, because C IV ionization time is long, the delay between peak 1600 Å and peak 171 Å is actually a lower limit.

We then employ a model for the cooling of the plasma based on that of Cargill, Mariska, & Antiochos (1995), which takes into account both conductive and radiative cooling. The conductive cooling time is given by $4 \times 10^{10}\, nL^2 T^{-5/2}$, and the radiative cooling time is given by $3kT^{1-\alpha}/n\chi$, where n and T are density and temperature in the loop, L is the loop half-length (in our case, loop length was about 25″), and α and χ are parameters in the radiative loss function $P = \chi T^{\alpha}$. For short, dense loops such as these the cooling time is dominated by the radiative component. We estimate the density of the 171 Å (assumed $\log T = 6$) plasma to be about 10^{10} cm^{-3} (calculated from emission measure and temperature), with a filling factor of 0.1. With this temperature and density the radiative cooling time is short, about 80 s; thus, with cadence of 35 s, the loops may cool though the passband rapidly, within a single exposure. This illuminates somewhat the mystery of why there are no obvious signs of cooling after the initial heating event.

Although these events are prevalent throughout the *TRACE* observations made during the last few years, they remain an enigma. Further study is clearly warranted. One of the most important questions that remains is whether these events are the EUV counterparts to ARTBs. Unfortunately, high-cadence SXT data taken at the same time do not overlap our field, and thus we cannot determine whether the brightenings we see correlate with ARTBs. Further active region observations with *TRACE* and SXT may answer this question. *TRACE*'s broad database of previous observations contains similar high-cadence observations that coordinate many different wavelengths. A look back at these data may further elucidate this question. Simultaneous observations at several different temperatures, with higher cadence and, preferably, with higher spatial resolution, would be also very helpful in answering these questions.

TRACE is supported by contract NAS5-38099 from NASA to LMATC. The authors are grateful to Harry Warren for many enlightening discussions.

REFERENCES

Berghmans, D., & Clette, F. 1999, Sol. Phys., 186, 207
Berghmans, D., McKenzie, D., & Clette, F. 2001, A&A, 369, 291
Cargill, P. J., Mariska, J. T., & Antiochos, S. K. 1995, ApJ, 439, 1034
Forbes, T. G., & Acton, L. W. 1996, ApJ, 459, 330
Golub, L., et al. 1999, Phys. Plasmas, 6, 2205
Handy, B. N., et al. 1999, Sol. Phys., 187, 229
Lin, R. P., Schwartz, R. A., Kane, S. R., Pelling, R. M., & Hurley, K. C. 1984, ApJ, 283, 421
Moses, D., et al. 1997, Sol. Phys., 175, 571
Scherrer, P. H., et al. 1995, Sol. Phys., 162, 129
Schrijver, C. J. 2001, Sol. Phys., 198, 325
Schrijver, C. J., et al. 1999, Sol. Phys., 187, 261
Shimizu, T. 1994, in X-Ray Solar Physics from *Yohkoh*, ed. Y. Uchida (Tokyo: Universal Academy Press), 33
Shimizu, T., Tsuneta, T., Title, A., Tarbell, T., Shine, R., & Frank, Z. 1996, in IAU Colloq. 153, Magnetodynamic Phenomena in the Solar Atmosphere: Prototypes of Stellar Magnetic Activity, ed. Y. Uchida, T. Kosugi, & H. S. Hudson (Boston: Kluwer), 37
Warren, H. P., Bookbinder, J. A., Forbes, T. G., Golub, L., Hudson, H. S., Reeves, K., & Warshall, A. 1999, ApJ, 527, L121